orano TLI

LTR-20000-160-03

8161 Maple Lawn Blvd
Suite 480
Fulton, Maryland 20759
☎ 1 301 421 4324
1 301 421 4326

June 17, 2022

ATTN: Document Control Desk,
Director, Division of Spent Fuel Management,
Office of Nuclear Material Safety and Safeguards,
U.S. Nuclear Regulatory Commission,
Washington, DC 20555-0001

Dear Director:

Orano TLI hereby submits the response to the Request for Additional Information (RAI), issued on May 3, 2021, for Revision 13 to the Versa-Pac Safety Analysis Report (SAR), Docket No. 71-9342. The response to the RAI is documented in Attachment 1 to this letter and Revision 13 of the Versa-Pac SAR with change pages resulting from the RAI Response are also enclosed in this submittal. Change pages in the SAR are marked 'June 2022' in the header and a summary of all changes is provided in Attachment 2 to this letter. The affidavit for withholding from public disclosure is documented in LTR-20000-130-04, submitted jointly with this application along with a redacted version of the updated SAR.

In addition to the changes to the SAR due to RAI responses, this submittal includes one requested clarification to the NRC Certificate of Compliance (CoC) and minor changes to the Versa-Pac Licensing Drawing based on manufacturer and customer feedback to improve the fabrication process. The requested change to the Versa-Pac NRC CoC is the explicit allowance for natural thorium in TRISO fuel compacts, under 5/(b)(1)(ii). The changes to the Licensing Drawing include:

1. **Sheet 1, Notes**:
   a) Added Note 19 to supplement Note 5 and clarify the use of threaded inserts for repair.
   b) Added Note 20 to clarify that the name plate may be welded or riveted to the drum. This was already included in Note 5 of Section 1.4.2 in the SAR, but not explicitly on the licensing drawing. (Note call out added on Sheet 1 – Section A7)
   c) Revise Note 21 to allow optional handles to be added to the drum lid for simpler handling. (Note call out added on Sheet 1 – Section C5)
2. **Sheet 1 – Section B7**: Changed lid plug dimensions to reflect tolerance stack up and made diameter a reference dimension.
3. **Sheet 2 – Section D1**: Revised part BB-2 thread call out to agree with Note 5.

4. **Sheet 2 – Section D3**: Removed MT weld inspection requirement between parts PG (top plate ring) and DA (drum body). This is the last weld on the package where the 55-gallon drum outer skin is welded on to the packaging structure. This weld does not perform any safety significant function, so an MT inspection on the weld is not required. As with all other welds during fabrication, a visual inspection of this weld is still required.

In addition to the requested revisions to the Versa-Pac CoC, Orano TLI also requests a five-year renewal of the certificate. Currently, the Versa-Pac Certificate 9342 expires in May of 2024. To avoid the need for an additional renewal application in the near future, an extension of the license based on a five-year renewal term is requested.

To support customer scheduling obligations, we request the approval of the certificate revision by the end of August 2022. Orano TLI is committed to providing timely responses to any proposed questions to support this timing.

Thank you for your attention to this license application for the Versa-Pac. This report is being submitted in accordance with 10CFR71.1, Communications and records. The enclosures of this report are being submitted through the EIE system.

Please address any questions or comments to the undersigned.

Sincerely,

Digitally signed by Philip Sewell
Date: 2022.06.17 15:09:43 -04'00'

Philip Sewell
Principal Nuclear Engineer
Orano TLI

Email: *psewell@tliusa.com*
Work: *(301) 421-4066*
Cell: *(301) 514-6567*

Non-Proprietary Enclosures:

Description:	File Name:
Affidavit to Withhold Proprietary Information	LTR-20000-160-04.pdf
SAR Revision 13, Non-Proprietary	VP SAR Rev 13-NP.pdf

Proprietary Enclosures:

Description:	File Name:
SAR Revision 13, Proprietary	VP SAR Rev 13-P.pdf

Attachment 1 – RAI Responses

NRC RAI 2-1

Demonstrate how the dynamic structural responses of the Versa-Pac 55 (VP-55) transportation package for the center-of-gravity (C.G.) over the bottom corner drop orientation are bounded by the dynamic structural responses of the bottom-end and side drop orientations.

In SAR Section 2.12.2.2 "Method of Analysis," of the SAR, the applicant stated that four package orientations were considered for the evaluations of the VP-55 package under the normal conditions of transport and hypothetical accident conditions free drops: (i) bottom-end, (ii) top-end, (iii) side, and (iv) C.G. over top-corner. However, the applicant provided a statement in the section without providing any explanations, "A drop with the c.g. over the bottom corner is bounded by the bottom-end and side drop orientations and is therefore not evaluated." Provide explanations of how the responses of the C.G. over the bottom corner drop are bounded by the responses of the bottom-end and side drops.

This information is needed by the staff to determine compliance with 10 CFR 71.41(a) and 10 CFR 71.55(d)-(e).

Orano TLI Response:

The C.G. over bottom corner cases are added to the SAR. Figure 2-1.1 shows the model coordinate system with the NCT and HAC results presented in Table 2-1.1 and Table 2-1.2, respectively. Review of the results shows that the component accelerations are bounded by the bottom-end and side drop cases. Additionally, because of the lid geometry, the top-end C.G. over corner drop bounds the bottom-end C.G. over corner results. Further discussion is provided in the response to RAI 2-2.

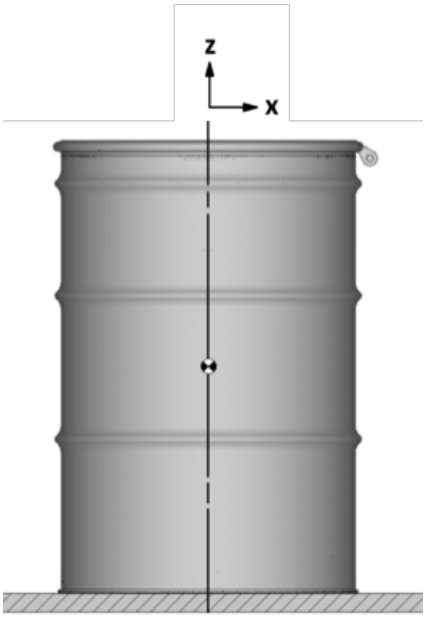

Figure 2-1.1. Model Coordinate System

Table 2-1.1. NCT 4-ft Free Drop VP-55 Package Contents Peak Acceleration

Package Drop Orientation	Thermal Condition	Absolute Peak Rigid Body Acceleration (g)	
		X-Direction	Z-Direction
Bottom-End	Cold	---	105
	Hot	---	104
Top-End	Cold	---	111
	Hot	---	43
Side	Cold	121	---
	Hot	105	---
C.G. over Top-Corner	Cold	99	109
	Hot	73	56
C.G. over Bottom-Corner	Cold	90	96
	Hot	76	93

Table 2-1.2. HAC 30-ft Free Drop VP-55 Package Contents Peak Acceleration

Package Drop Orientation	Thermal Condition	Absolute Peak Rigid Body Acceleration (g)	
		X-Direction	Z-Direction
Bottom-End	Cold	---	394
	Hot	---	381
Top-End	Cold	---	208
	Hot	---	355
Side	Cold	515	---
	Hot	403	---
C.G. over Top-Corner	Cold	321	334
	Hot	284	306
C.G. over Bottom-Corner	Cold	272	268
	Hot	202	259

NRC RAI 2-2
Demonstrate the following:

a) The applicant provided the calculated peak accelerations of the package in SAR Tables 2-8 and 2-9 from the results of the LS-DYNA finite element (FE) analyses. a) SAR Table 2-8 shows that all peak accelerations of the Cold/Hard Form are larger than the peak accelerations of the Hot/Soft Foam for each orientation. However, SAR Table 2-9 shows that the peak accelerations of the Cold/Hard Form are smaller than the peak accelerations of the Hot/Soft Foam for the Top-End and C.G. over Top-Corner orientations.

b) For the use of Cold/Hard Form, the largest acceleration (133 g) was obtained with the C.G. over Top-Corner orientation in SAR Table 2-8, while the largest acceleration (515 g) was obtained with the side orientation in SAR Table 2-9. However, when the Hot/Soft Foam was used, the largest acceleration (105 g) was obtained with the side orientation in SAR Table 2-8, while the largest acceleration (422 g) was obtained with the C.G. over Top-Corner orientation in SAR Table 2-9. Provide: (a) explanations of the effects of the orientation and material properties with respect to the VP-55 performance under normal conditions of transport and hypothetical accident conditions free drops, and (b) technical justifications that the LS-DYNA analyses are accurate and consistent.

This information is needed by the staff to determine compliance with 10 CFR 71.41(a) and 10 CFR 71.55(d)-(e).

Orano TLI Response:
While the use of the cold/hard foam properties produces higher accelerations than do the hot/soft foam properties for the NCT top-corner impact as would be expected, this is not the case for the HAC top-corner impact as originally presented. This unexpected phenomenon is caused by how the different foam properties allow the mock contents to interact with the closure mechanism of the VP-55 Inner Container.

During the HAC top-corner impact simulation with hot/soft foam properties, the ceramic blanket surrounding the Inner Container (modeled as foam) and the Containment Insulation Plug does not provide as much support to the Inner Container Containment Body as the foam with cold/hard foam properties. This allows the corner of the simulated contents to deform the Containment Body to such an extent that it pinches the Containment Body between it and the Inner Container threaded insert, which is part of the Inner Container closure mechanism. This metal-to-metal interaction results in higher accelerations to the simulated contents.

During the HAC top-corner impact simulation with cold/hard foam properties, the ceramic blanket surrounding the Inner Container (modeled as foam) provides enough support to the Inner Container Containment Body to allow the simulated contents to slide along the Containment Body—directing it to the Containment Insulation Plug, which provides additional cushioning to the contents. This keeps the Containment Body from being pinched between the simulated contents and the Inner Container threaded insert—resulting in lower accelerations to the simulated contents.

Figure 2-2.1 presents the deformation of the package near the Inner Container closure mechanism at times during the analyses when the simulated contents had reached its lowest point before rebounding. As can be seen in this figure, there is more deformation of the Inner Container Body with it being pinched between the simulated contents and Inner Container threaded insert.

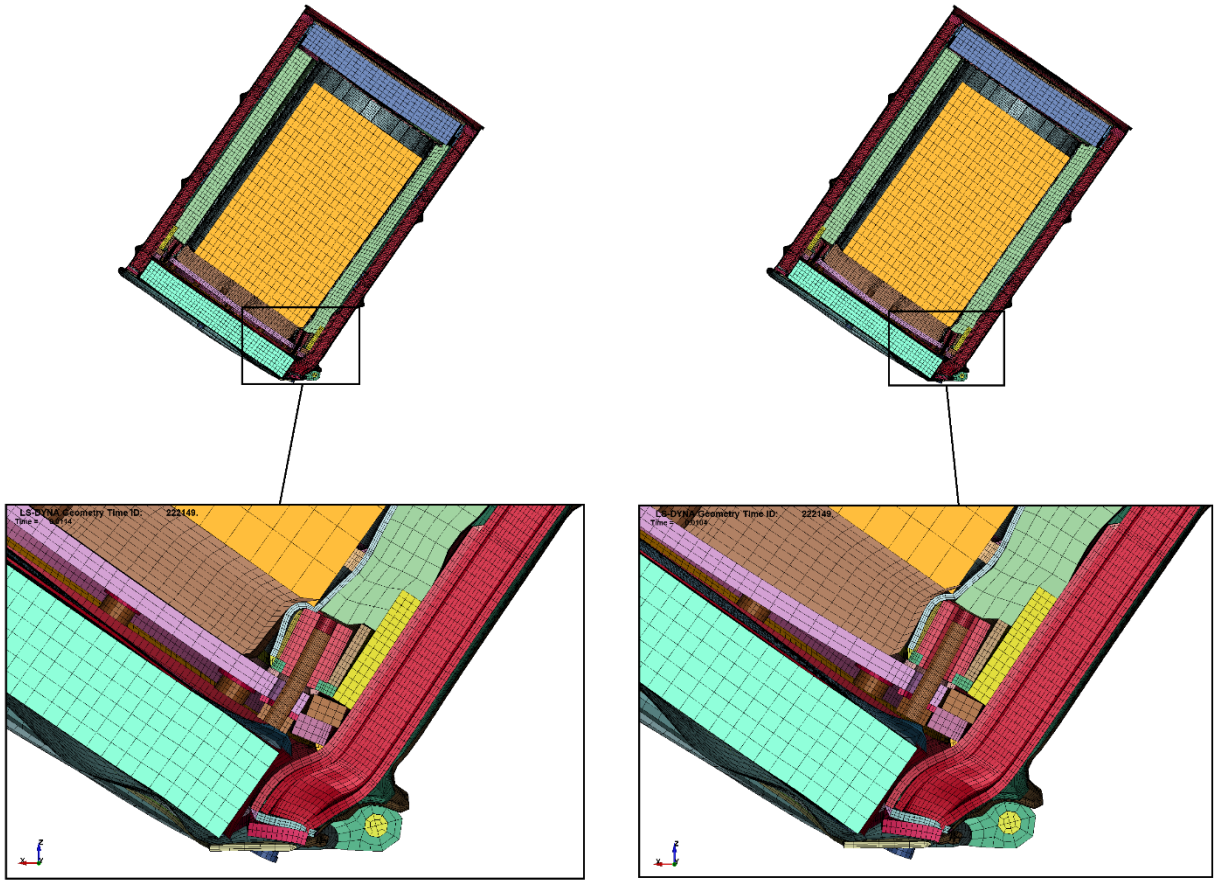

Figure 2-2.1. HAC Top-Corner Impact Simulation—Comparison of Hot/Soft and Cold/Hard Foam Properties

For the re-analysis of the top corner drops, the simulations are performed (NCT and HAC) with the package aligned to the global coordinate system such that the global z-axis is the long axis of the package. This improves the post-processing of the acceleration results and provides a better comparison with the side and end drop cases presented in Tables 2-1.1 and 2-1.2 of the response to RAI 2-1.

The mock contents are positioned within the package cavity as initially resting on the Containment Insulation Plug rather than having them initially resting on the Containment End Plate as shown in Figure 2-2.2. This was done so that the updated top-corner impact simulations will better compare to an actual drop test. As shown in Tables 2-1.1 and 2-1.2, positioning the mock contents in this initial position within the package cavity eliminates the phenomenon where the contents experience a higher acceleration during hot conditions than cold conditions.

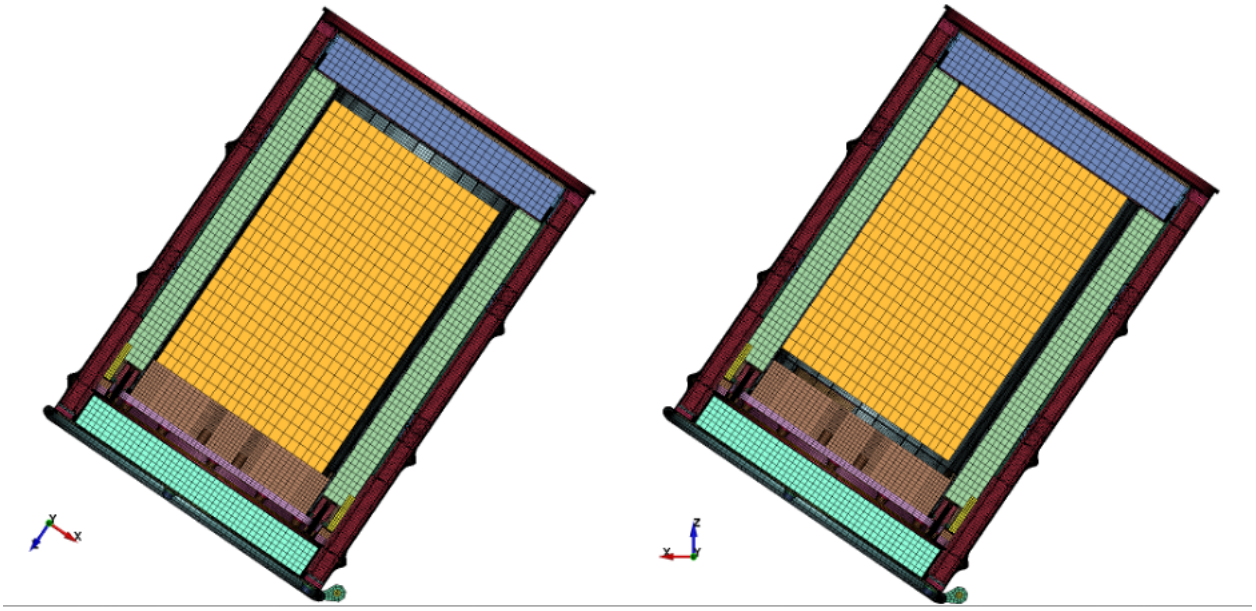

Figure 2-2.2. Top-Corner Impact Simulation—Comparison of Initial Position of the Mock Contents

NRC RAI 2-3

The applicant provided a FE model for the High-Capacity Basket (HCB) in SAR Section 2.12.3.3, "Finite Element Model Description." Provide the following:

a) Explain the statement of "with bounded contact," in SAR Section 2.12.3.3,

b) Provide details of how the bolt and its connection were modeled,

c) ANSYS contact elements were used for interactions between components. Explain how friction was treated for the contact elements and what criteria were used to determine a status of fixed, friction and free condition during an impact,

d) If a fixed condition was used between components, provide technical justifications whether or not the ANSYS analyses provide conservative responses, and

e) Provide a benchmark study that demonstrates the validity of the ANSYS numerical analyses to accurately predict responses of the HCB by physical model test.

This information is needed by the staff to determine compliance with 10 CFR 71.41(a) and 10 CFR 71.55(d)-(e).

Orano TLI Response:

Question a:

The statement "with bounded contact" is a typographical error. The statement should read "with bonded contact". However, for clarity, the SAR is revised using the wording of the response to Question b below.

Question b:
As shown in Figure 2-3.1, Bonded contact is used between the bolts and connecting rods, and threaded rods and hex nuts. Frictional contact is used between bolts and disks, hex nuts, and stiffener arms. No separation contact is used between the threaded rods and stiffener arms and connecting rods and disks.

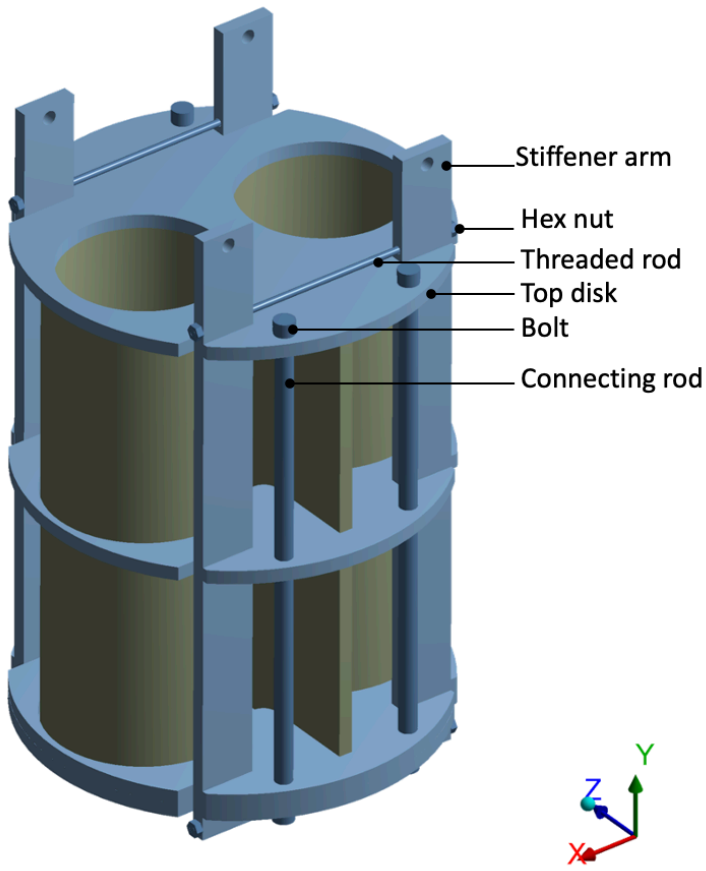

Parts Connected	Contact type
Bolt + Connecting rod	Bonded
Bolt + Top disk	Frictional
Threaded rod + Hex nut	Bonded
Hex nut + Stiffener arm	Frictional
Threaded rod + Stiffener arm	No separation
Connecting rod + disks	No separation

Figure 2-3.1. HCB ANSYS Model Contact Details

Question c:

Bonded contact is used between threaded rods and nuts, and between connecting rods and bolts. No separation contact is used between stiffening arm and support disks and connecting rods and support disks. Frictional contact is used between bolts and disks, hex nuts, and stiffener arms, and CPVC and disks. Where frictional contacts are used between CPVCs, and CPVC and aluminum parts, a friction constant of 0.4 is used based on the maximum static friction of plastic materials, whereas for aluminum and steel, a friction constant of 0.61 is used based on the maximum static friction of steel-aluminum friction combinations provided in Reference [1].

To determine the contact angle for the side-drop case between the HCB and VP-55 inner shell, the LS-DYNA side drop results were reviewed. The results show that as the rigid mass presses against the thin inner shell (10 ga = 0.135 inch), the shell flexes and conforms to the shape of the contents. For HCB side drop model, compression-only support is applied on the impact side of the support disks up to the slot for the stiffener arm. Figure 2-3.2 shows the ANSYS model and coordinate system. For stability, a single node is also constrained at the centerline of each side drop case that prevents the model from spinning and sliding.

For the end drop, compression-only support is applied to the bottom impact surface of the four stiffening arms, and the bottom surface of the bottom disk where it is supported by a foam pad. In addition, a rotation constraint is applied at the center line to prevent the model from spinning.

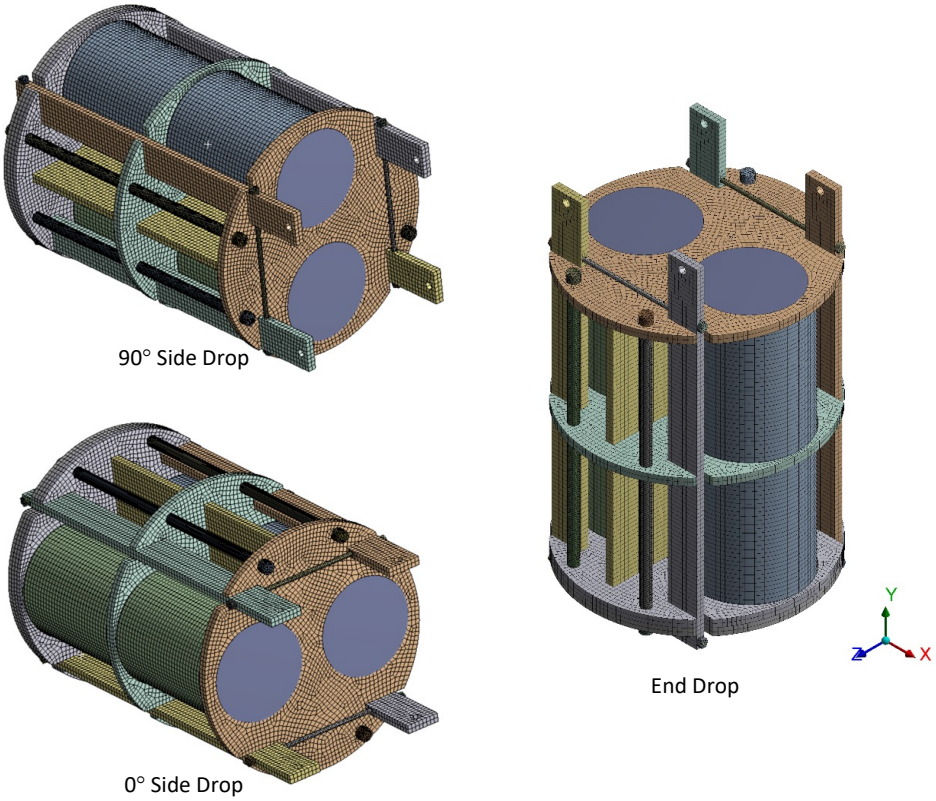

Figure 2-3.2. HCB ANSYS Model Drop Orientations

Question d:
Compression-only supports are used to simulate drop conditions. As explained in the Question c response, a single node is constrained for numerical stability by preventing spinning and lateral displacements of the model without affecting the stress results.

Question e:
To further the development of internal components such as the HCB, an accurate LS-DYNA model of the VP-55 with rigid contents was developed. The goal of the LS-DYNA analysis is to obtain acceleration results (see response to RAI 2-1), which can then be used as input for pseudo-static ANSYS analyses of the internal components. Therefore, to verify the accuracy of the acceleration results, benchmarking of the LS-DYNA is performed by comparing the analysis cases with the corresponding test results.

Since 2009, the Versa-Pac has been subjected to approximately 20 individual physical drop tests to develop and refine the design. In October 2017, the maximum gross weight of the package was increased to 750 pounds and was dropped in orientations that most challenged the lid closure. The sequence included 4-ft and 30-ft corner drops, side drop/dynamic crush, and puncture to the lid center.

Figure 2-3.1 shows a comparison of the 30-foot top corner drop that targeted the drum closure ring. Review of the drop test results shows that the LS-DYNA accurately predicts damage to the drum closure. Figure 2-3.2 compares the HAC pin puncture test with the LS-DYNA results. Review of the results show good agreement between the test and analysis results with the post-test damage geometry the same.

To capture the effects of cumulative damage, Figure 2-3.3 shows the Versa-Pac damage following the 30-foot side drop and dynamic crush test sequence. This sequence was chosen to challenge the internal support structure, which historically is the weak link in drum package designs, e.g., failure of the historic DOT spec 6M drum to pass the dynamic crush test. Following the side drop and dynamic crush sequence, the drums chines were flattened on both sides, absorbing a significant amount of the impact energy. Little ovalization of the structure occurred with the drum closure remaining in position. Comparison of the overall damage shows good agreement between the test and LS-DYNA test sequence results.

Because the drop test and LS-DYNA results compared favorably, there is a high level of confidence that the rigid body acceleration results accurately represent the response of the Versa-Pac during NCT and HAC. Therefore, applying these accelerations to the pseudo-static ANSYS model of the HCB accurately predicts the response of the structure.

Figure 2-3.1. HAC Top-Corner

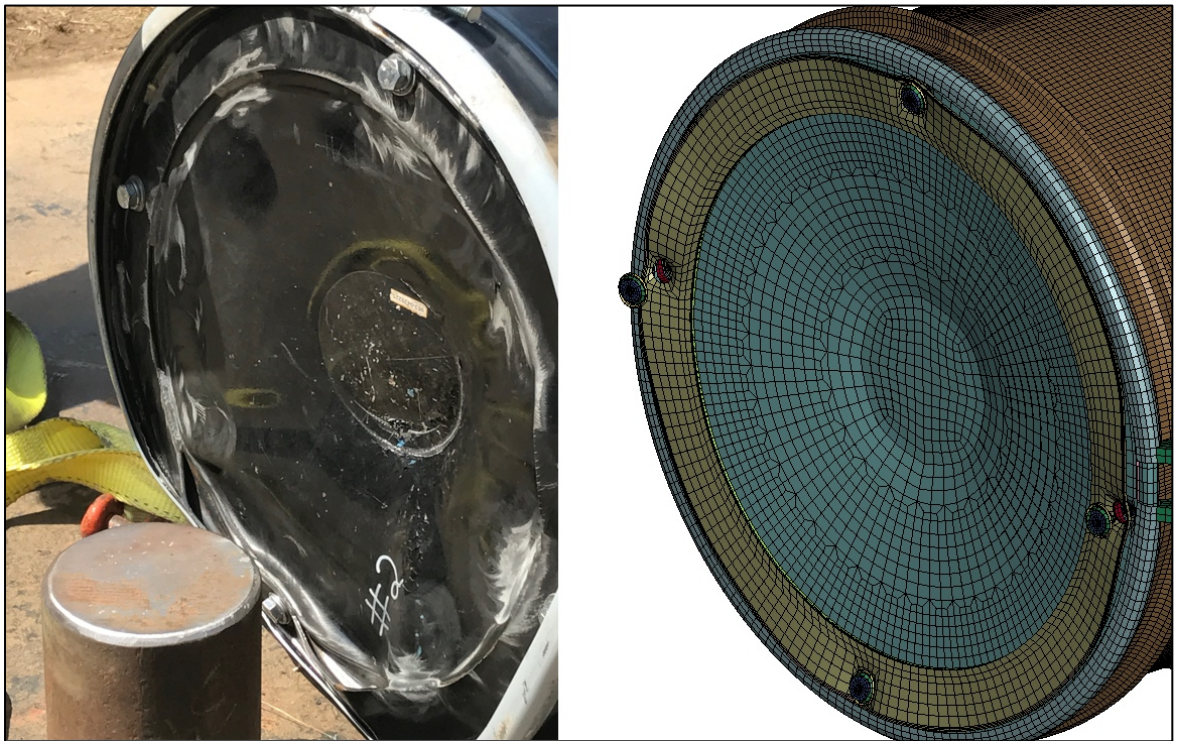

Figure 2-3.2. Top 30-ft Free-Drop/Crush/Puncture

Figure 2-3.3. Side 30-ft Free-Drop/Crush

NRC RAI 2-4

Provide the following information for the HCB stress analysis with the hypothetical accident conditions end drop:

a) the maximum induced bending and shear stresses in the basket,

b) the minimum margin of safety in the basket,

c) technical assumptions made for the basket stress analysis, and

d) buckling analysis and its results for the elastic stability of the basket.

This information is needed by the staff to determine compliance with 10 CFR 71.41(a), 10 CFR 71.55(d)-(e), and 10 CFR 71.73(c)(3).

Orano TLI Response:

Question a and b:

The maximum induced bending and shear stresses in the basket are presented in Table 2-4.1 below.

Table 2-4.1. Maximum Induced Bending and Shear in HCB

Stress Type	Maximum Stress (ksi)	Allowable Stress (ksi)	Minimum Design Margin
Bending	3.7	14.7	+2.97
Shear	2.2	17.6	+4.59

Notes:
Bending allowable: 50% of Pm allowable = 0.5 × 0.7Su = 14.7 ksi, where Su = 42ksi.
Shear allowable: 0.42Su = 17.6 ksi, where Su = 42ksi.

Question c:

Technical assumptions made for the basket stress analysis:

- Mechanical properties are taken at upper bound temperatures of 200°F and 150°F for the steel and CPVC components, respectively. Basis: The HCB is inside the Versa-Pac. The maximum NCT temperature of the Versa-Pac cavity is 138°F. These temperatures also apply to the initial conditions for the HAC free drop.
- NCT and HAC top end and bottom corner drops are bounded by NCT and HAC bottom end and side drops. Basis: For NCT the accelerations do not vary significantly, however, only the bottom end and side drops carry the HCB content weight. The side HAC drop acceleration (515 g) and bottom end drop accelerations (394 g) are higher than the top end drop (209 g) and top corner drop (352 g). During the corner drop, the vectored impact load is divided between the end and side of the HCB and is less than the individual end and side drop cases (see response to RAI 2-1). Therefore, it is expected that the bottom end and side drop stresses bound of the top end and bottom corner drop stresses.
- The moderator pipes and separator plate are modeled for content placement only. Basis: Structural support for the HCB is provided by aluminum disks, stiffener arm frames, tie rods, and threaded rods. The moderator pipes and separator plate are captured by the support disk, top disk, and bottom disk.

Question d:
Buckling analysis and its results for the elastic stability of the basket:

An ANSYS eigenvalue non-linear buckling analysis of the HCB is documented using the bottom end impact pre-stress. The results show that the load multiplier eigenvalue for the lowest buckling mode is 13.6.

The factor of safety against buckling of the HCB for the bottom end drop is equal to the eigenvalue for the lowest mode, or 13.6. Per section F-1331.5 of the ASME Appendix F [2], the stress is limited to 2/3 of the buckling stress. Therefore, the margin of safety against buckling of the HCB for the HAC bottom end drop is:

$$M.S. = (2/3 \times 13.6) - 1.0 = +8.07$$

NRC RAI 7-1

Provide additional details in the drawing for the new HCB to specify the temper of the Aluminum 6061 material.

Drawing VP-55-HCB indicates materials composed of “Aluminum 6061.” The mechanical properties used in the structural analysis of the HCB are consistent with a specific temper of that material (ASTM B209 6061-T6). Absent additional detail in the drawing to define this specific temper designation, it is unclear to the staff how procurement will be controlled to ensure that a different temper 6061 material is not used that could result in a nonconservative structural analysis.

This information is needed to determine compliance with the requirements of 10 CFR 71.33(a)(5) and 71.35(a).

Orano TLI Response:

The licensing drawing is revised to show the specific temper of the aluminum material is ASTM B209 6061-T6.

NRC RAI 7-2

Clarify if the mechanical properties of the chlorinated polyvinyl chloride (CPVC) are credited in the structural analysis of the package. If so, provide additional information on how these values were determined.

SAR Table 2-26, "Structural Properties of CPVC," provides the strength and other materials properties of the CPVC moderating material. However, it is unclear to what extent the CPVC is relied on to support a mechanical load during accident conditions. Also, the staff was unable to verify the properties provided for CPVC based on the referenced source provided in the SAR. For example, there appear to be small differences in the tensile yield strength and more significant differences in elastic modulus between the SAR data and the source document. Should these properties be relied on in the SAR, staff requests additional information to allow verification of the accuracy of the properties provided for CPVC in the SAR.

This information is needed to determine compliance with the requirements of 10 CFR 71.33(a)(5) and 71.35(a).

Orano TLI Response:

As stated in the response to RAI 2-4(c), the moderator pipes and separator plate are modeled for content placement only. Structural support for the HCB is provided by aluminum disks, stiffener arms frames, tie rods, and threaded rods. The moderator pipes and separator plate are captured by the support disk, top disk, and bottom disk. However, during the side drop the bearing stresses are evaluated at the points of contact with the contents. The bearing stress for the 90° side drop results in a peak bearing stress of 5.0 ksi, which is less than the tensile strength of the material at 150°F. Therefore, the CPVC will remain in position following HAC. This result supports the criticality analysis conservative assumption that 50% of the CPVC remains following HAC.

The properties presented in Table 7-2.1 have been verified and expanded and, for some properties, multiple references are provided where manufacturer data is unavailable. For consistency, the stress analyses are updated with the revised properties.

Table 7-2.1. Structural Properties of CPVC (revised SAR Table 2-27)

Property, units	Value at Temperature, °F (°C)				Reference
	73 (22.8)	120 (48.9)	150 (65.6)	180 (82.2)	
Tensile Strength S_U, psi (MPa)	8000 (55.2)	6352 (43.8)	5300 (36.5)	4248 (29.3)	[3], p5.2
Modulus of Elasticity E, ksi (MPa)	423.0 (2916)	355.0 (2448)	309.5 (2134)	269.0 (1855)	[3], p4.9
Mean Coefficient of Thermal Expansion, α, E-6, in/in/°F (E-6, m/m/°C)	0.34 (0.612)				[3], p4.8
Poisson's Ratio	0.386				[4], [5]
Density, lbm/in³ (g/cm³)	0.056 (1.55)				[3], p5.1

NRC RAI 7-3
(Editorial) The staff reviewed the mechanical properties provided for the bolts in Section 2.12.2.4.5 of the SAR and identified a typographical error (12,000 psi rather than 120,000 psi as indicated in the cited reference for SAE J429 Grade 5 bolts). The staff requests correction of this error.

Orano TLI Response:
Typographical error corrected.

NRC RAI 7-4

Resolve apparent discrepancies between the thermal properties of the Rockboard and CPVC and the cited references. In addition, provide Reference 19 of Chapter 3, which is not readily available.

SAR Tables 3-23 and 3-24 provide the material properties used in the thermal analyses for the Rockwool Rockboard and CPVC, respectively. The staff were unable to verify the values provided by the applicant. For example, the cited reference for the Rockboard does not contain the values in the SAR. Also, the staff were unable to recreate the thermal property values for the CPVC using the cited technical data sheet (Reference 18).

This information is needed to determine compliance with the requirements of 10 CFR 71.33(a)(5) and 71.35(a).

Orano TLI Response:

Additional references are added to the SAR to clarify the thermal properties for Rockwool Rockboard 60 provided in Table 7-4.1 and CPVC in Table 7-4.2, which are also provided as attachments to this letter following the complete bibliography. Reference numbers will be updated once the official SAR tables are revised.

The thermal conductivity value is from the referenced technical data sheet [6]. However, the value must be calculated from the RSI (thermal resistance value) provided. The RSI value is given as 0.75 m²K/W for 25.4 mm (0.0254 m) thickness. Taking the inverse of the RSI and multiplying the thickness, the thermal conductivity is calculated to be 0.034 W/m·K. To benchmark this value, a comparison was made to thermal property data available in open literature. From Reference [7], p2-12, data is provided for Rockwool Mineral Fiber in the same density range. The calculated value compares favorably with the results presented in the table. The specific heat is taken from the CRC Handbook of Thermal Engineering (Reference [8], Table C.1), which provides thermal properties for Mineral Wool Blanket of the same density. The temperature limit is taken from Reference [9], p20. Below is Table 7-4.1 with reference column added.

Table 7-4.1. Thermal Properties of Rockwool Rockboard 60 (revised SAR Table 3-23)

Property, units	Temperature, °F[°C]	Reference
	75 [24]	
Density, lbm/ft³ [kg/m³]	6 [96]	[6]
Thermal Conductivity, BTU·in/hr·ft²·°F [W/(m·k)]	0.236 [0.034]	[6], RSI = 0.75 m²K/W @25.4 mm
Specific Heat, BTU/lbm·°F [kJ/kg·K]	0.2 [0.837]	[8], Table C.1
Temperature Limit, °F[°C]	482[250]	[9], p20

Thermal properties for CPVC used in the HCB thermal analysis are obtained from [3]. Temperature limits for the pipe and sheet grade materials are from reference [10]. Below is Table 7-4.2 with reference column added.

Table 7-4.2. Thermal Properties of CPVC (revised SAR Table 3-24)

Property, units	Value at Temperature, °F (°C)		Reference
	73 (23)	212 (100)	
Density, lbm/ft^3 [g/cm^3]	96.8 [1.55]	---	[3], p3.2
Thermal Conductivity, BTU·in/hr·ft^2·°F [W/(m·k)]	0.95 [0.137]	---	[3], p3.2
Specific Heat, BTU/lbm·°F [kJ/kg·K]	0.21 [0.90]	0.26 [1.10]	[3], p3.2
Temperature Limit F° (°C), Pipe Grade	248-291 (120-144)		[10]
Temperature Limit F° (°C), Sheet Grade	241-248 (116-120)		

NRC RAI 7-5

Update the SAR, as applicable, to evaluate the potential for chemical, galvanic, or other adverse reactions for the new HCB materials.

The addition of the HCB introduces several new materials to the internal environment of the transportation package, such as 6061 aluminum, Rockwool Rockboard insulation, stainless steel, and CPVC piping and sheets. Existing language in SAR Section 2.2.2 discuss material compatibility, but this section has not been updated to address new potential combinations of materials and any resulting reactions. Confirm whether statements such as "the compatibility of materials and the combination of these materials has been demonstrated not to experience significant material loss due to chemical and galvanic reactions" and "all of the insulation materials have low chloride content" remain valid and that no additional considerations are needed for the added materials of the HCB.

This information is required to verify compliance with 10 CFR 71.43(d).

Orano TLI Response:

Additional discussion is added to SAR Section 2.2.2 that discusses the compatibility of the HCB materials of construction and the Versa-Pac. The HCB is constructed of aluminum, stainless steel, CPVC and Rockwool.

Stone wool (Rockwool®) insulation is inorganic, and will not rot, corrode, or promote fungi or bacteria growth and is compatible with aluminum, stainless steel, and painted surfaces. Stone wool maintains its dimensional integrity under all conditions. Rockwool is non-combustible and has a high melting point of 2150 °F (1177 °C) and does not produce toxic smoke in the event of a fire. Corzan® CPVC is resistant to over 400 chemicals and compounds including all varieties of aluminum. CPVC is a stable material and is not subject to leaching of chlorides. Because stone wool and CPVC are often used in industrial applications subjected to environmental conditions, no chemical or galvanic reaction is expected with other components of the HCB.

Bibliography

[1] STRUCT, "Static Friction Coefficients," Web: https://structx.com/Material_Properties_005a.html, Accessed, Dec. 10, 2021.

[2] American Society of Mechanical Engineers(ASME), "Boiler and Pressure Vessel Code - Rules for Construction of Nuclear Facility Components," Section III, Division I - Appendices.

[3] Corzan Industrial System, "Engineering Design Manual - Basic Physical Properties," Noveon, Inc., Cleveland Ohio, 2002.

[4] SHIMADZU, "Measurement of Poisson's Ratio and Elongation for Polyvinyl Chloride (PVC)," https://www.shimadzu.com/an/industries/engineering-materials/film/poisson/index.html, 2022.

[5] HARVEL, "PVC & CPVC Corrosion Resistant Industrial Pressure Pipe, Physical Properties of PVC & CPVC," Gorge Fischer Harvel LLC, Easton PA, 2012.

[6] ROCKWOOL, "ROCKBOARD® 40/60/80, Premium Multipurpose Board Insulation for Acoustic/Thermal Applications," ROCKWOOL, Milton, Ontario Canada, 2022.

[7] U.S. Department of Commerence - National Bureau of Standards, "An Assessment of Needs for New Thermal Reference Materials," NBSIR 85-3146, Gaithersburg, MD, 1985.

[8] F. Kreith, Handbook of Thermal Engineering, Boca Raton, FL: CRC Press, 2000.

[9] ROXUL, Inc., "Rockwool Technical Insulation Process Manual," RW-TI/10.19/Eur-Am/Int ENG 410, Milton, ON Canada.

[10] M. L. Knight, "Corzan Industrial Systems: Response to Technical Inquiry," 19 August 2021.

Attachment 2 – Summary of SAR Change Pages

The following table is provided to supplement the submittal and aid review by outlining all changes made to Revision 13 of the Versa-Pac SAR due to RAI responses. The SAR revision remains Rev. 13, but the changed pages list the date of the new submittal (June 2022) rather than that of the original submittal (December 2021). The SAR page, table, and figure numbers listed in the table below match the numbering in the new SAR submittal, for instances where pages, tables, and/or figures were inserted and subsequent numbering has been changed. Note on the change pages that revision bars are retained for all Revision 13 changes, whether the change was in the original or new submittal.

SAR Page	Change Description
i-iii	- Updated Record of revisions table to list revisions added for RAI Response change pages
1-6	- Revised contents description under Section 1.2.2 to list natural thorium as an acceptable material for general contents (first paragraph) and TRISO compacts (second paragraph)
1-12 to 1-13	- Revised VP-55 licensing drawing (VP-55-LD, Rev.6)
1-26	- Revised High Capacity Basket licensing drawing (VP-55-HCB-LD, Rev.1)
2-i to 2-v	- Updated table of contents and lists of tables and figures
2-7 to 2-8	- Added discussion of chemical and galvanic reactions to SAR Section 2.2.2
2-32	- Reference [33] listing revised but reference remains the same. Addition of references [34] and [35] to Section 2.12.1. Prior references [34] and [35] renumbered to [36] and [37], respectively.
2-33 to 2-34	- Revision of Tables 2-8 and 2-9 to add C.G. over bottom corner results and break out lateral and axial accelerations. Editorial change to 2.12.2.2 to remove wording stating that c.g. over bottom corner drop is not evaluated.
2-35	- Revised Figure 2-1 to show C.G. over bottom corner drop orientation
2-45	- Revised sentences 3 and 4 of Section 2.12.2.6 for clarification. Revised Table 2-18 to add C.G. over bottom corner results and break out lateral and axial accelerations
2-55	- Section 2.12.2.6.4 discussion revised to clarify method and break out axial and lateral accelerations results
2-56 to 2-57	- Updated Figures 2-18 through 2-21 for updated results. Figure 2-19 now shows deflection of blind flange. Figure 2-20 now shows x-axis, z-axis, and total accelerations.
2-58 to 2-60	- Added Section 2.12.2.6.5 to document NCT C.G. over bottom corner results

2-61	- Revised Table 2-19 to add C.G. over bottom corner results and break out lateral and axial accelerations
2-62 to 2-70	- Only Page, Table, and/or Figure numbering changed due to insertions above. Header still shows 'December 2021' due to no change in page content.
2-71	- Section 2.12.2.7.4 discussion revised to clarify method and break out axial and lateral accelerations results
2-72 to 2-73	- Updated Figures 2-38 through 2-41 for updated results. Figure 2-39 now shows deflection of blind flange. Figure 2-40 now shows x-axis, z-axis, and total accelerations.
2-74 to 2-76	- Added Section 2.12.2.7.5 to document HAC C.G. over bottom corner results
2-77	- Only Page, Table, and/or Figure numbering changed due to insertions above. Header still shows 'December 2021' due to no change in page content.
2-78 to 2-79	- Discussion in Section 2.12.3.1 updated to include new results. Results summary including Table 2-20 through 2-23 updated for new results based on RAI response changes. Added Table 2-24.
2-80	- Clarification to last sentence in Section 2.12.3.3
2-81	- Only Page, Table, and/or Figure numbering changed due to insertions above. Header still shows 'December 2021' due to no change in page content.
2-82	- Revised Table 2-27 to show references for CPVC material and include additional temperature data.
2-83	- Only Page, Table, and/or Figure numbering changed due to insertions above. Header still shows 'December 2021' due to no change in page content.
2-84	- Table 2-29 updated to include bending stress criteria. Table 2-30 numbering updated due to insertion of tables above.
2-85 to 2-87	- Only Page, Table, and/or Figure numbering changed due to insertions above. Header still shows 'December 2021' due to no change in page content.
2-88 to 2-89	- Result values in tables updated.
2-90	- Sections 2.12.3.9 and 2.12.3.10 added to document HCB buckling and CPVC bearing stress evaluations.
3-30	- HCB component references [20] – [23] added to Section 3.5.1
3-58	- Tables 3-23 and 3-24 updated to list the specific reference and location of the thermal properties for the Rockboard® and CPVC HCB components